

Dynamics of Surfactant-Suspended Single-Walled Carbon Nanotubes in a Centrifugal Field

Nitish Nair,^{†,§} Woo-Jae Kim,^{†,§} Richard D. Braatz,[‡] and Michael S. Strano^{*,†}

Department of Chemical Engineering, Massachusetts Institute of Technology, Cambridge, Massachusetts 02139, and Department of Chemical and Biomolecular Engineering, University of Illinois at Urbana-Champaign, Urbana, Illinois 61801

Received August 14, 2007. In Final Form: October 11, 2007

A hydrodynamic model is used to describe the motion of surfactant-suspended single-walled carbon nanotubes in a density gradient, while being subjected to a centrifugal field. The number of surfactant molecules adsorbed on each nanotube determines its effective density and, hence, its position in the gradient after centrifugation has been completed. Analysis of the spatial concentration distributions of CoMoCAT nanotubes suspended with 2 w/v% sodium cholate yielded 2.09, 2.14, and 2.08 surfactant molecules adsorbed per nanometer along the length of the (6,5), (7,5), and (8,7) nanotubes, respectively. The estimates are commensurate with experimental values reported in the literature and can be used to predict the fate of sodium cholate-suspended nanotubes in the separation process. Since the density of the surfactant–nanotube assembly is highly sensitive to the number of adsorbed molecules, a perturbation would cause it to be enriched at a different location in the gradient. The level of sensitivity is also reflected in the 95% confidence levels that are reported in this work.

Introduction

The successful suspension of single-walled carbon nanotubes (SWNTs) in water was made possible by the use of the surfactant sodium dodecyl sulfate (SDS) and ultracentrifugation to remove bundles from the sample.¹ The centrifuge-based separation of CoMoCAT SWNTs by diameter and electronic structure was recently achieved by suspension with bile salts such as sodium cholate (SC).² Previous efforts involved DNA as the suspension agent.³ The extent of adsorption of the surfactant on nanotubes of varying chiralities is not uniform, and creates assemblies with different buoyant densities. This facilitates their separation by isopycnic centrifugation, where particles migrate to regions of like density. The selective enrichment of certain (*n,m*) SWNTs was demonstrated by either tuning the pH of the solution or by using SDS as a cosurfactant.² It is important to understand these phenomena at the molecular level so that further improvements to the process can be made.

The sedimentation of solute molecules in a solvent during ultracentrifugation is modeled by the Lamm equation.⁴ The temporal and spatial distribution of particles in the centrifuge tube is determined by competing diffusive and sedimentation fluxes. Analytical solutions of the Lamm equation, based on certain simplifications, are available^{5–11} but involve the calcula-

tion of functions that are too complex to fit to experimental data. With advances in computing power over the years, it has been possible to numerically simulate the trajectories of particles during centrifugation. Such simulations reduce the number of assumptions and allow the inclusion of nonlinearities that would otherwise preclude closed-form answers. The first numerical solution of the Lamm equation was performed using finite element methods by Claverie et al.¹² Later work extended the scope of this technique to the sedimentation of molecules in dynamic density gradients¹³ and compressible media,¹⁴ among other cases.^{15,16}

In this work, we seek to use the theory of the centrifuge^{6,17} and the numerical analysis of the Lamm equation to describe the motion of surfactant-suspended SWNTs in a density gradient, and estimate the number of surfactant molecules adsorbed per unit length of the nanotube. The latter determines the density of the SWNT–surfactant assembly, and, although we cannot discern how it depends on chirality, we now have a bound for the number of species on the SWNT surface. It has been noted that this technique of separating suspended nanotubes with the centrifuge is purely density-based² and does not depend on their velocities in the gradient. We have accounted for the sedimentation of the gradient material and the solvent compressibility due to the high speed of rotation, since both factors determine the final positions of the enriched fractions.

Experimental Section

SWNT Preparation. Two types of nanotubes were used in this study: CoMoCAT SWNTs (Southwest Nanotechnologies, Inc.) for separation by diameter, and HiPco SWNTs (HPR 162.3, Rice University) for separation by electronic type. Suspension of SWNTs in water with 2 w/v% SC was performed by ultrasonication and ultracentrifugation to obtain individual nanotubes as described in the literature.² In both cases, the concentration of SWNTs was adjusted

* Corresponding author. E-mail: strano@mit.edu.

[†] Massachusetts Institute of Technology.

[‡] University of Illinois at Urbana-Champaign.

[§] These authors contributed equally to this work.

(1) O'Connell, M. J.; Bachilo, S. M.; Huffman, C. B.; Moore, V. C.; Strano, M. S.; Haroz, E. H.; Rialon, K. L.; Boul, P. J.; Noon, W. H.; Kittrell, C.; Ma, J. P.; Hauge, R. H.; Weisman, R. B.; Smalley, R. E. *Science* **2002**, *297*, 593.

(2) Arnold, M. S.; Green, A. A.; Hulvat, J. F.; Stupp, S. I.; Hersam, M. C. *Nat. Nanotechnol.* **2006**, *1*, 60.

(3) Arnold, M. S.; Stupp, S. I.; Hersam, M. C. *Nano Lett.* **2005**, *5*, 713.

(4) Lamm, O. *Ark. Mat. Astr. Fys.* **1929**, *21B*.

(5) Faxen, H. *Ark. Mat. Astr. Fys.* **1929**, *21B*, 1.

(6) Fujita, H. *Mathematical Theory of Sedimentation Analysis*; Academic Press: New York, 1962.

(7) Holladay, L. A. *Biophys. Chem.* **1979**, *10*, 187.

(8) Philo, J. S. *Biophys. J.* **1996**, *72*, 435.

(9) Behlke, J.; Ristau, O. *Biophys. J.* **1997**, *72*, 428.

(10) Archibald, W. J. *Phys. Rev.* **1938**, *53*, 746.

(11) Archibald, W. J. *J. Appl. Phys.* **1946**, *18*, 362.

(12) Claverie, J.; Dreux, H.; Cohen, R. *Biopolymers* **1975**, *14*, 1685.

(13) Schuck, P. *Biophys. Chem.* **2004**, *108*, 187.

(14) Schuck, P. *Biophys. Chem.* **2004**, *108*, 201.

(15) Schuck, P. *Biophys. J.* **1998**, *74*, 466.

(16) Schuck, P. *Biophys. J.* **1998**, *75*, 1503.

(17) Svedberg, T.; Pedersen, K. O. *The Ultracentrifuge*; Oxford University Press: Oxford, 1940.

to 1 mg/mL. SWNT solution was first homogenized for 1 h at 65 000 rpm (T18 basic ultra-turrax, IKA) and then sonicated for another hour with a 1/8" probe tip at 10 W (130 W ultrasonic processor, Cole-Parmer). The resulting solution was centrifuged for 1 h at 22 °C and 32 000 rpm to eliminate bundles and nonsuspended nanotubes (Optima L-100XP centrifuge, Beckman Coulter). SWNTs prepared in this way were used in the separation steps described below.

Diameter Separation. Separation of CoMoCAT SWNTs by diameter in a density gradient was performed as described in the literature.² The gradient was made using a non-ionic medium, OptiPrep (60 w/v% iodixanol, Sigma-Aldrich), in a linear density gradient maker (SG30, Hoefer, Inc.). The resulting density of the solution ranged from 7.5 to 22.5 w/v%, with a total volume of 8 mL. One milliliter of CoMoCAT SWNT (density = 20 w/v%) was injected at the bottom of the gradient and centrifuged for 22.26 h at 22 °C and 32 000 rpm using a swinging bucket SW 32.1 Ti rotor (Beckman Coulter). After centrifugation, SWNT samples were fractionated at every 150 μ L in a fraction recovery system (Beckman Coulter), and characterized by UV-visible-near-infrared (UV-vis-NIR) absorption spectroscopy (Shimadzu UV-310PC absorption spectrometer) to investigate the extent of enrichment of specific SWNT diameters.

Electronic-Type Separation. The separation of HiPco SWNTs into metallic or semiconducting fractions was performed according to the protocol² to separate laser-ablation-grown nanotubes. Surfactant mixtures of SDS and SC in a weight ratio of 3:2 for metallic SWNT enrichment and 1:4 for semiconducting SWNT separation were utilized.² The density gradient also contained the same mixture of SDS and SC. The solution density ranged from 20 to 35 w/v% and 15 to 30 w/v% for the metallic and semiconducting SWNT separations, respectively. One milliliter of HiPco SWNT, having the same ratios of surfactant mixtures by the addition of 2 w/v% SDS in water, was injected at the bottom of each density gradient. The density of the injected SWNT solution was 32.5 w/v% and 27.5 w/v% in the 3:2 and 1:4 cases, respectively. All the other conditions were similar to the diameter separation described above.

Model Development

SWNT Concentration Profiles. The one-dimensional Lamm equation for the concentration distribution ($C_{(n,m)}$) of an (n,m) nanotube in a sector-shaped cell,^{4,6,10,17} as a function of its diffusion coefficient ($D_{(n,m)}$) and sedimentation velocity ($u_{(n,m)}$) is

$$\frac{\partial C_{(n,m)}}{\partial t} = \frac{D_{(n,m)}}{r} \frac{\partial}{\partial r} \left(r \frac{\partial C_{(n,m)}}{\partial r} \right) - \frac{1}{r} \frac{\partial}{\partial r} (r C_{(n,m)} u_{(n,m)}) \quad (1a)$$

The origin lies at the center of the centrifuge rotor, and all distances along the radial coordinate (r) are expressed relative to it. The above partial differential equation (PDE) is solved with a finite volume method, using a first-order upwind scheme for the sedimentation term.¹⁸ The particle velocity is determined by the competing forces of centrifugation and hydrodynamic drag. To reduce the complexity of the system, we assume that the velocity field reaches equilibrium well before the concentration field. The velocity in terms of the SWNT mass ($M_{(n,m)}$), angular velocity of the rotor (ω), friction coefficient ($f_{(n,m)}$), solution density (ρ_s), and particle density ($\rho_{(n,m)}$) is

$$u_{(n,m)} = \frac{M_{(n,m)} \omega^2 r}{f_{(n,m)}} \left[1 - \frac{\rho_s}{\rho_{(n,m)}} \right] \quad (1b)$$

We define velocity explicitly instead of including it in the sedimentation coefficient, which is not constant for each SWNT

and varies radially due to the nonuniform density.^{19–21} The orientationally averaged friction coefficient, $f_{(n,m)}$, is obtained by approximating the nanotube as a circular cylinder composed of a stack of rings:^{22–26}

$$f_{(n,m)} = \frac{3\pi\eta L_{(n,m)}}{\ln \left[\frac{L_{(n,m)}}{d_{(n,m)}} \right] + 0.32} \quad (1c)$$

where $L_{(n,m)}$ and $d_{(n,m)}$ are the SWNT length and diameter, respectively, and η is the viscosity of the aqueous solution, which is assumed to change negligibly with pressure.²⁷ Supposing that the nanotubes in solution do not interact with each other, the (n,m) frictional and diffusion coefficients can be related by the Einstein–Smoluchowski equation:^{28,29}

$$f_{(n,m)} = \frac{kT}{D_{(n,m)}} \quad (1d)$$

The diffusion coefficients are taken to be independent of the solute concentration. At high values of the latter, the Lamm equation ceases to be applicable.³⁰

Surfactant–SWNT Density. The density of the surfactant–nanotube assembly ($\rho_{(n,m)}$) can be described by a single parameter, namely, the number of surfactant molecules adsorbed per unit length of the SWNT (n_s). For a specific (n,m) species, the number of carbons per nanometer (n_c) can be estimated,^{31,32} and when combined with n_s , yields the total mass per unit length ($M_{(n,m)}$):

$$M_{(n,m)} = \sum_j n_{s,j} M_{s,j} + n_c M_c + n_f M_f + n_{\text{sol}} M_{\text{sol}} \quad (2a)$$

where M_s (M_c) is the molecular (atomic) weight of surfactant (carbon), and the summation is carried out over all the surfactants in solution. The last pair of terms is applicable when the interior of the nanotube is filled with either n_f molecules (per nanometer) of a fluid with molecular weight M_f , or n_{sol} molecules (per nanometer) of the solvent with molecular weight M_{sol} . The general formula for the volume per unit length of the assembly is

$$V_{(n,m)} = \sum_j n_{s,j} V_{s,j} + \frac{\pi}{4} d_{\text{eff}}^2 - n_{\text{sol}} V_{\text{sol}} \quad (2b)$$

$$d_{\text{eff}} = d_{(n,m)} + 2r_c \quad (2c)$$

where r_c is the van der Waals radius of a carbon atom in aromatic molecules (~ 1.72 Å).³³ The third term in eq 2b is a correction when the interior of the SWNT is accessible to the solvent whose molar volume is V_{sol} . In this work, we have assumed that the pores in the SWNT lattice are devoid of any fluid, i.e., $n_f = n_{\text{sol}}$

(19) Schumaker, V. N.; Rosenbloom, J. *Biochemistry* **1965**, *4*, 1005.

(20) Schumaker, V. N.; Rosenbloom, J. *Biochemistry* **1967**, *6*, 1149.

(21) Dishon, M.; Weiss, G. H.; Yphantis, D. A. *Biopolymers* **1971**, *10*, 2095.

(22) Bloomfield, V.; Dalton, W. O.; Van Holde, K. E. *Biopolymers* **1967**, *5*, 135.

(23) de la Torre, J. G.; Bloomfield, V. A. *Biopolymers* **1977**, *16*, 1747.

(24) McCammon, J. A.; Deutch, J. M. *Biopolymers* **1976**, *15*, 1397.

(25) Planken, K. L. Monodisperse DNA restriction fragments Part II: Sedimentation velocity and sedimentation equilibrium. Undergraduate Thesis, Utrecht University, Utrecht, The Netherlands, 2003.

(26) Tirado, M. M.; de la Torre, J. G. *J. Chem. Phys.* **1979**, *71*, 2581.

(27) Bett, K. E.; Cappi, J. B. *Nature* **1965**, *207*, 620.

(28) Zwanzig, R.; Bixon, M. *Phys. Rev. A* **1970**, *2*, 2005.

(29) Islam, M. A. *Phys. Scr.* **2004**, *70*, 120.

(30) Mashimo, T. *Phys. Rev. A* **1988**, *38*, 4149.

(31) Saito, R.; Dresselhaus, G.; Dresselhaus, M. S. *Physical Properties of Carbon Nanotubes*; Imperial College Press: London, 1998.

(32) Cabria, I.; Mintmire, J. W.; White, C. T. *Phys. Rev. B* **2003**, *67*, 121406.

(33) Kitaigorodskii, A. I. *Org. Kristalloghim.* **1955**, 558.

(18) Leveque, R. J. *Finite Volume Methods for Hyperbolic Problems*; Cambridge University Press: Cambridge, U.K., 2002.

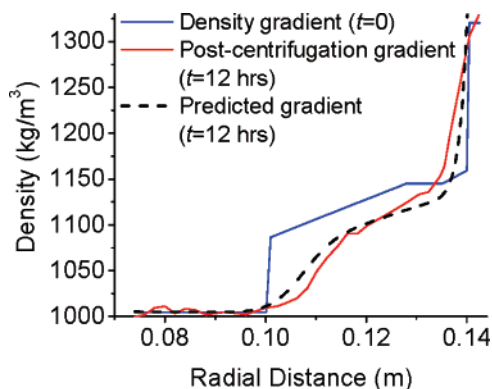


Figure 1. The original density gradient (blue) changes after centrifuging for 12 h (red) due to the sedimentation of iodixanol. The solution of the Lamm equation predicts the final density profile (black), and a comparison with the experimental data gives the diffusion coefficient of iodixanol (D_I) as $\sim 2.5 \times 10^{-10} \text{ m}^2/\text{s}$.

= 0. Additionally, the nanotubes are presumed to be uncapped and lacking catalyst particles. Values of the anhydrous molar volumes of the surfactants under study (V_s)^{34–36} were found in the literature. Anhydrous surfactant molecules impart little, if any, buoyancy to the nanotubes. We have therefore accounted for one hydration shell while calculating the apparent molar volumes of SC ($\sim 613 \text{ mL/mol}$) and SDS ($\sim 403 \text{ mL/mol}$) using approximate hydration numbers for each.^{37,38} Finally, the buoyant density of a generic nanotube is

$$\rho_{(n,m)} = \frac{M_{(n,m)}}{V_{(n,m)}} \quad (2d)$$

Dynamic Density Gradient. The concentration of the density gradient material, iodixanol, changes in space and time due to sedimentation, leading to a variation in the solution density (ρ_s).¹³ The iodixanol molecules settle according to eq 1a, with the subscript (n,m) replaced by I . The motion of the gradient in the centrifugal field is assumed to be independent of the cosolute (SWNT).³⁹ Instead of solving the PDEs for the nanotubes and iodixanol simultaneously, a look-up table containing the sedimentation profiles of the gradient at different times was created beforehand. During the computation of the SWNT trajectories, the instantaneous density gradient was obtained by interpolation from the tabulated values. The diffusion coefficient of iodixanol (D_I) was calculated by comparing the theoretically predicted gradient profile with data collected by Arnold et al.² (Figure 1), and was found to be $\sim 2.5 \times 10^{-10} \text{ m}^2/\text{s}$.

Solvent Compressibility. The compressibility of water (κ) is so low ($4.6 \times 10^{-10} \text{ Pa}^{-1}$) that it is considered incompressible at ordinary pressures. However, the tremendous forces generated by centrifugation lead to pressures that are high enough to affect the solution density. The radial dependence of pressure (P) is given by¹⁴

$$dP = \rho_s \omega^2 r dr \quad (3a)$$

Combining eq 3a with the definition of compressibility,

$$d\rho_s = \kappa \rho_s dP \quad (3b)$$

a relation between the densities of successive cells in the computation domain can be obtained:

$$\rho_{s,i+1} = \frac{\rho_{s,i}}{1 - \alpha \rho_{s,i}} \quad (3c)$$

where $\alpha = (\kappa \omega^2 / 2)(r_{i+1}^2 - r_i^2)$. In this pair of equations, i denotes the i th cell in the discretized space. The density in the first cell ($\rho_{s,1}$) is simply that of water at atmospheric pressure. We have considered the compressibility of the iodixanol–water solution to be the same as that of pure water.

Time Scale. The length-dependent time scale for each (n,m) entity ($\tau_L^{(n,m)}$) is determined by the interplay of the hydrodynamic drag and centrifugal force:

$$\tau_L^{(n,m)} = \frac{f_{(n,m)}}{M_{(n,m)} L_{(n,m)} \omega^2} \quad (4)$$

In the denominator of eq 4, the SWNT length ($L_{(n,m)}$) appears because the total mass of the nanotube system is used to calculate the centrifugal force. For the CoMoCAT sample, a Gaussian length distribution was used with parameters that were obtained for DNA–SWNT assemblies separated by centrifugation,³ while for HiPco, a log-normal abundance profile was assumed.⁴⁰ Centrifugal forces have a smaller effect on short nanotubes as compared to longer ones, since their masses are lower. In the density gradient, the former travel slower but diffuse to a greater extent than the latter.

Results and Discussion

Assumptions. Monolayer coverage of the surfactant on the SWNT is assumed while calculating the density of the assembly. In the presence of a cosurfactant, both species are thought to adsorb at different sites on the nanotube so that the total volume equals the sum of the component volumes. A conclusive visualization of SDS adsorbed on SWNTs is yet to be articulated. SDS has been shown to form cylindrical micelles,¹ beads,⁴¹ hemimicelles,⁴² and, more recently, random, structureless features⁴³ on SWNT surfaces. We have adopted the last formulation in determining the total surfactant volume. The estimation of n_s is contingent on the assumption that the SWNT is pristine, and can be constructed by a simple axial translation of the unit cell. End effects have been neglected. The use of a single parameter (n_s) for a separated fraction implies the uniform adsorption of surfactants on the corresponding nanotube surface. In other words, each (n,m) species has a single density, not a range.

Diffusion plays a secondary role while the nanotubes are moving through the gradient in a centrifugal field. However, its effect will be greater during the start-up and shut-down phases of the centrifuge. We have neglected these regimes in the computation. It is not clear whether the density gradient is linear as soon as it is injected into the centrifuge tube. The evolution

(34) Brun, T. S.; Hoiland, H.; Vikingstad, E. *J. Colloid Interface Sci.* **1977**, *63*, 89.

(35) Szabo, G. H.; Hoiland, H. *Langmuir* **1998**, *14*, 5539.

(36) Smith, W. B.; Barnard, G. D. *Can. J. Chem.* **1981**, *59*, 1602.

(37) Hayter, J. B.; Penfold, J. *Colloid Polym. Sci.* **1983**, *261*, 1022.

(38) Messina, P.; Morini, M. A.; Schulz, P. C. *Colloid Polym. Sci.* **2003**, *281*, 695.

(39) Sartory, W. K.; Halsall, H. B.; Breillatt, J. P. *Biophys. Chem.* **1976**, *5*, 107.

(40) Usrey, M. L.; Nair, N.; Agnew, D. E.; Pina, C. F.; Strano, M. S. *Langmuir* **2007**, *23*, 7768.

(41) Islam, M. F.; Rojas, E.; Bergery, D. M.; Johnson, A. T.; Yodh, A. G. *Nano Lett.* **2003**, *3*, 269.

(42) Richard, C.; Balavoine, F.; Schultz, P.; Ebbesen, T. W.; Mioskowski, C. *Science* **2003**, *300*, 775.

(43) Yurekli, K.; Mitchell, C. A.; Krishnamoorti, R. *J. Am. Chem. Soc.* **2004**, *126*, 9902.

of the gradient with time has been calculated by approximating linearity at the start of the run.

The critical micelle concentration (cmc) and solubility of a surfactant are affected by pressure.^{44,45} A change in the cmc can be neglected because of the excess quantities of surfactants used to suspend SWNTs. The solubility of SDS in water drops drastically above 1000 atm.⁴⁴ Calculations indicate that pressures in the region of interest (the density gradient) do not exceed this value.⁴⁶ A similar analysis could not be performed for SC because of the lack of information regarding the effect of pressure on its solubility in water.

Separation Using SC. The diameter-based separation of CoMoCAT nanotubes using centrifugation is conceptually the easiest to describe mathematically, since only one surfactant (2 w/v% SC) is involved. The model has been applied to data generated during the course of this work and in the literature.² We use relative SWNT concentrations as defined by Arnold et al.,² wherein the (n,m) concentrations are normalized to the corresponding maxima. The two datasets differ in the rotor configuration, centrifuge tube dimensions, and centrifugation time. The final SWNT positions (Figures 2a,b) and gradient profiles⁴⁶ differ in both cases. However, the result that we seek (n_s , the number of SC molecules adsorbed per nanometer) should be similar, as is evident in Table 1, which shows n_s with its 95% confidence limits.⁴⁷ The radial SWNT concentration curves from the Arnold dataset are approximate, and this could adversely affect the comparison. In the original work,² the distribution of each fraction was given in terms of densities. The spatial equivalent had to be extracted from the predicted density gradient after 12 h of centrifugation.

Earlier measurements of SDS coverage on SWNT yielded 2–3 molecules/nm².^{48,49} The surface coverage of sodium dodecylbenzene sulfate was at least 8 times higher than that of SDS.⁵⁰ Such a high packing density might be due to adsorption along the tube followed by the “tails-on” configuration.^{50,51} Our estimates of SC adsorption on an areal basis are listed in Table 1. The values for SC surface coverage are lower than those of SDS because of the larger molar volume of the former. The diameter and length of the cholic acid molecule are roughly 0.6 and 1.32 nm, respectively.⁵² It is plausible that at least two cholate molecules can adsorb onto the SWNT surface within a linear distance of 1 nm.

We have also collected data for different run times of the 2 w/v% SC–SWNT sample (12 h and 44.53 h) in order to check the veracity of the coverage estimates. The final SWNT concentration profiles were situated close to the point of injection. In the case of the 12 h sample, this was because the nanotubes had not been given sufficient time to move upward. For the 44.53 h sample, the extended run time meant that the SWNT had reached their respective isopycnic points and were carried downward by the sedimenting density gradient. Either way, it was not possible to obtain data that were as clean as the 22.26 h sample, since the bulkier tubes at the bottom have high

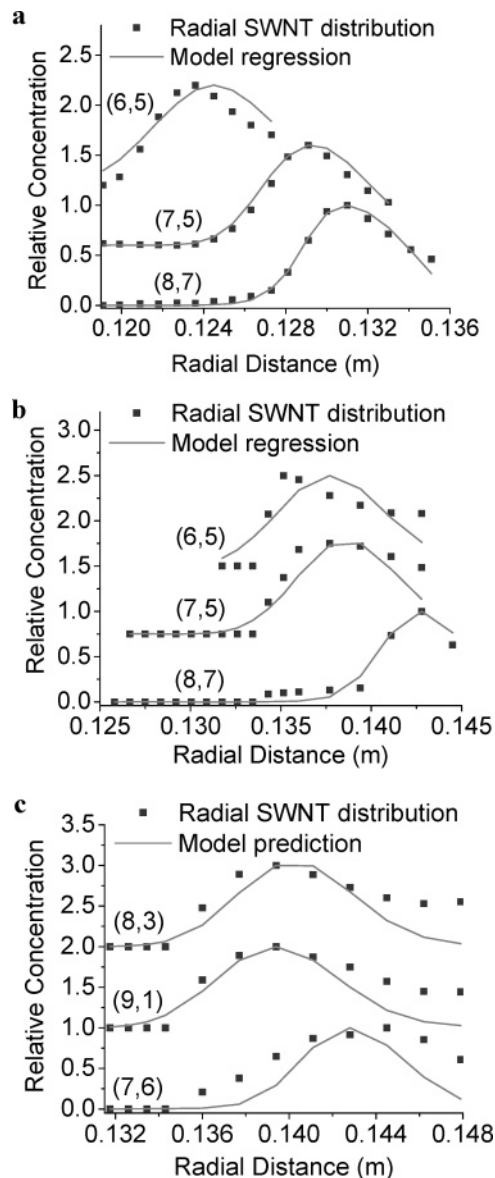


Figure 2. Diameter separation of CoMoCAT SWNTs using 2 wt % SC in (a) the work of Arnold et al. and (b,c) this work. Panels a and b show the final concentration distributions of three semiconducting SWNTs along the length of the centrifuge tube. As nanotube diameters increase, so do their masses and buoyant densities, which yields enrichment at different radial positions. (c) Predicted concentration profiles for the (8,3), (9,1), and (7,6) nanotubes. All the plots have been offset for clarity.

Table 1. Comparison of the Fit Parameter (n_s) for Three Semiconducting SWNTs in Two Datasets Involving SC, and the Corresponding Buoyant Densities^a

SWNT	n_s (molec/nm)	lower limit	upper limit	areal basis ^b (molec/nm ²)	density (kg/m ³)
(6,5)	2.1229	2.1038	2.1601	0.6138	1060.3
	2.0955	2.0611	2.1294	0.6058	1063.6
(7,5)	2.0003	1.9920	2.0074	0.5428	1085.2
	2.1382	2.1247	2.1560	0.5802	1068.7
(8,7)	2.0076	1.9988	2.0120	0.4644	1094.9
	2.0753	2.0638	2.0865	0.4801	1087.4

^a From the work of Arnold et al. (bold) and the present work (Roman).

^b The nominal value of n_s on an areal basis. Relative to the corresponding numbers for SDS, SC has much lower coverage values, probably due to its larger size.

absorbances and artificially raise the concentrations of the SWNTs of interest. The approximate profiles for the (6,5) and (7,5)

(44) Tanaka, M.; Kaneshina, S.; Tomida, T.; Noda, K.; Aoki, K. *J. Colloid Interface Sci.* **1973**, *44*, 525.

(45) Hamann, S. D. *J. Phys. Chem.* **1962**, *66*, 1359.

(46) See Supporting Information.

(47) Beck, J. V.; Arnold, K. J. *Parameter Estimation in Engineering and Science*; John Wiley and Sons, Inc.: New York, 1977.

(48) Grossiord, N.; van der Schoot, P.; Meuldijk, J.; Koning, C. E. *Langmuir* **2007**, *23*, 3646.

(49) Strano, M. S.; Moore, C. M.; Miller, M. K.; Allen, M. J.; Haroz, E. H.; Kittrell, C.; Hauge, R. H.; Smalley, R. E. *J. Nanosci. Nanotechnol.* **2003**, *3*, 81.

(50) Matarredona, O.; Rhoads, H.; Li, Z.; Harwell, J. H.; Balzano, L.; Resasco, D. E. *J. Phys. Chem. B* **2003**, *107*, 13357.

(51) Cardenas, J. F.; Glerup, M. *Nanotechnology* **2006**, *17*, 5212.

(52) Sugihara, G.; Tanaka, M. *Hyomen* **1978**, *16*, 537.

nanotubes were extracted and fitted.⁴⁶ The values of n_s for the 12 h (44.53 h) runs are 1.815 (1.84) and 1.832 (1.89) molecules/nm, respectively, which are not identical to those in Table 1 but are still within 5–10% of the corresponding 22.26 h values. Ideally, the same number of adsorbed SC molecules should be able to describe the 12, 22.26, and 44.53 h datasets. However, the optimal value of the fit parameter, n_s , is very sensitive to factors such as the spatial location of the fractions in the centrifuge tube, the starting position of the SWNT sample, and its spread after being injected into the gradient. In addition, as mentioned previously, the proximity of the SWNT fractions to the bulk sample also skews the concentration profiles. We note that the values reported in this work are simply statistical averages of the SC population on the nanotube surface. There is a constant exchange of SC molecules from the nanotube to the solution due to the thermodynamic equilibrium that exists between the adsorbed, micellar, and free surfactant phases.⁵³

A more reliable test of n_s is against the concentration profiles of the (9,1), (8,3), and (7,6) nanotubes (Figure 2c). Since the fitted estimates of n_s are clustered around 2 molec/nm, the profiles for these three tubes were obtained by fixing n_s at 2.04 molec/nm. The predictions are not perfect, although they roughly capture the SWNT positions after 22.26 h of centrifugation. Note that the experimental concentration profiles for individual SWNT are extracted from the absorption spectra, and are therefore affected by the convolution with neighboring spectral peaks.⁵⁴

Separation Using SDS–SC Mixtures. Tuning the SDS/SC weight ratio has resulted in the enrichment of semiconductors (surfactant ratio = 1:4) and metals (surfactant ratio = 3:2), most prominently in the case of laser-ablation-grown SWNTs.² HiPco samples have metallic and semiconducting species of comparable diameters. It is difficult to discern electronic separation in the case of HiPco nanotubes for two reasons: (i) tracking the absorption peak of a specific metal as an indicator of enrichment is not feasible because of the presence of semiconducting E_{22} peaks in the same spectral region, and (ii) metallic fractions in the centrifuged samples may also contain semiconductors with similar diameters. We have focused on the (6,5), (7,5), and (8,7) semiconducting nanotubes so that information obtained from the CoMoCAT fits can be used for the HiPco data. In other words, the n_s estimates from the single surfactant (SC) case provide a foundation for examining the dual surfactant (SDS–SC) scenario.

The fits of the 3:2 data (Figure 3a) show a diameter-based separation for semiconducting SWNTs, although their buoyant densities are observed to be higher than when SC alone is used (Table 2). The desorption of SC from the nanotube surface and its replacement by SDS, which has a lower molar volume, leads to an increase in density. The concentration profile for each semiconductor was fitted by assuming a 1:1 molecular displacement of SC by SDS, with the initial SC coverage already known from the CoMoCAT fits. While this may not be an accurate representation of reality, it does yield a lower bound for the SDS population on the nanotube. The analysis reveals the progressively greater uptake of SDS molecules (i.e., greater SC desorption) as SWNT diameter increases (Table 2). This is consistent with the higher activation energies required by SC to desorb from most small-diameter nanotubes.^{55,56} The ability of the 3:2 weight ratio

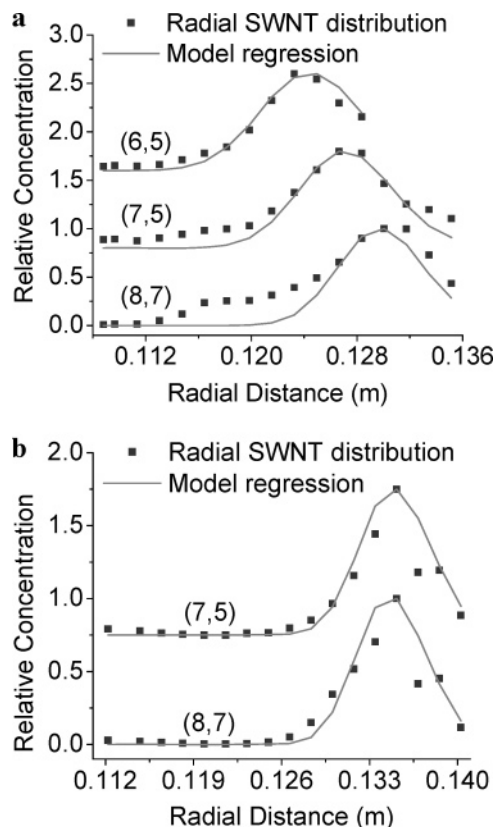


Figure 3. Concentration profiles for HiPco semiconducting SWNTs with (a) 3:2 SDS–SC weight ratio, and (b) 1:4 weight ratio. The fits assume that the total number of surfactant molecules adsorbed on the SWNTs is conserved. SDS is postulated to replace the already existing cholate, whose concentration on the nanotube surface is given by the analysis of the CoMoCAT diameter-separation data. The plots have been offset to improve clarity.

Table 2. Fit Parameters for Different SDS/SC Weight Ratios^a along with the Buoyant Densities of the HiPco SWNT–Surfactant Assemblies for Each Case

SWNT	$\{n_{\text{SDS}}, n_{\text{SC}}\}$ (molec/nm)	density (kg/m ³)
(6,5)	{0.6629, 1.4326}	1094.9
(7,5)	{0.8715, 1.2667}	1109
(8,7)	{0.8545, 1.2208}	1124.4
	{1.0643, 1.0739}	1119.1
	{0.7639, 1.3113}	1120.2

^a 3:2 (bold) and 1:4 (Roman).

to separate metals from semiconductors can be explained by the stronger interaction of SC with the former. Apart from the fact that cholate suspends more nanotubes as a result of its naphthenic structure,⁵⁷ the proximity of the hydroxyl groups in the cholate molecule to the nanotube surface results in electronic polarization toward the SWNT.⁵⁸ Metallic nanotubes have delocalized electrons at the Fermi level, and are more receptive to induced charges. Thus, metallic SWNTs have lower densities in the 3:2 case because of minimal SC desorption as compared to the semiconductors. In the case of large-diameter metals, it is also plausible that SDS adsorbs onto vacant areas on the surface and further reduces the density.

The 1:4 surfactant ratio leads to the enrichment of the (6,5) nanotube in the HiPco- and CoMoCAT-based runs (Figure 3b); however, the distribution of the (6,5) is too broad to be accurately

(53) Wang, H.; Zhou, W.; Ho, D. L.; Winey, K. I.; Fischer, J. E.; Glinka, C. J.; Hobbie, E. K. *Nano Lett.* **2004**, *4*, 1789.

(54) Nair, N.; Usrey, M. L.; Kim, W.-J.; Braatz, R. D.; Strano, M. S. *Anal. Chem.* **2006**, *78*, 7689.

(55) McDonald, T. J.; Engrakul, C.; Jones, M.; Rumbles, G.; Heben, M. J. *Phys. Chem. B* **2006**, *110*, 25339.

(56) McDonald, T. J.; Engrakul, C.; Jones, M.; Blackburn, J. L.; Rumbles, G.; Heben, M. J. *Proc. SPIE* **2005**, 5929, 59290W1.

(57) Tan, Y.; Resasco, D. E. *J. Phys. Chem. B* **2005**, *109*, 14454.

(58) Blackburn, J. L.; Engrakul, C.; McDonald, T. J.; Dillon, A. C.; Heben, M. J. *J. Phys. Chem. B* **2006**, *110*, 25551.

described by our model, and so, we have restricted parameter estimation to the (7,5) and (8,7) nanotubes (Table 2). Here, as expected, we observe that the increase in density can be accounted for by the adsorption of SDS in place of SC. Given the smaller amount of SDS present in the 1:4 surfactant solution as compared to 3:2, it is expected that its population on the SWNT surface will be correspondingly lower, which certainly is the case for the (8,7) nanotube (0.764 molec/nm versus 0.855 molec/nm). By this logic, there is an apparent discrepancy for the (7,5) species. At this juncture, we would like to emphasize that the 1:1 replacement of SC by SDS was assumed because of the lack of information involving any other adsorption scheme. It is entirely possible that not all the cholate molecules will be replaced by SDS, which still raises the density of the nanotube, while conforming to the approximate diameter dependence of SC desorption.^{55,56}

Finally, we have attempted to elucidate the effect of high pH on the isolation of small-diameter nanotubes.² The fits performed for the study at pH 8.5 for CoMoCAT nanotubes showed that the same n_s from Table 1 could be used to capture the profiles for the (6,5) and (8,7) SWNT.⁴⁶ The number of adsorbed SC molecules on the (7,5) increased from 2 molec/nm to 2.156 molec/nm. The preference of SC toward smaller nanotubes under high pH conditions can be explained as follows: The counterions (Na^+) of the surfactant are drawn away by the increased OH^- concentration in solution, which exposes the negatively charged headgroups (COO^-), raises intermonomer repulsions, lowers the aggregation number and, hence, the cmc. Under these circumstances, greater stability is offered by free surfaces in solution, namely, SWNTs. Because of the higher curvature of smaller diameter nanotubes, these charged surfactant molecules will tend to adsorb onto them in order to maximize the separation between their respective headgroups. These raised levels of adsorption on small-diameter SWNTs lower their densities and isolate them from their larger counterparts.

Conclusion

We have developed a model to describe the separation of surfactant-suspended SWNTs using centrifugation. Parameter estimates for the number of SC molecules adsorbed per unit nanotube length were obtained by fitting data in the literature as well as our own. The estimates, when converted to an areal basis, are less than those reported in past work for SDS but are still reasonable. This is expected, because of the relatively larger molar volume of the cholate molecule. We have also rationalized the 3:2 and 1:4 separation schemes, wherein the stronger interaction between SC and metallic SWNTs and the approximate diameter dependence of SC desorption from semiconducting nanotubes are significant in determining the respective buoyant densities.

Acknowledgment. This material is based upon work supported by the American Chemical Society Petroleum Research Grant (class G grant), Intel (class A grant), and the National Science Foundation under Award No. NIRT 0506660. M.S.S. is grateful for a Beckman Young Investigator Award. W.-J.K. is grateful for support by the Korea Research Foundation Grant funded by the Korean Government (MOEHRD) (KRF-2005-214-D00260). The authors would like to thank P. Barone and M. Usrey for useful discussions, and appreciate the clarifications provided by M. C. Hersam and M. S. Arnold with respect to their separation results.

Supporting Information Available: Figures corresponding to the model predictions for other semiconducting SWNTs, the 12- and 44.53-h runs, separation at high pH and using the 1:4 surfactant mixture, and plots of the calculated radial pressure distribution in the centrifuge tube. This information can be accessed free of charge via the Internet at <http://pubs.acs.org>.

LA702516U